RSC Advances

ROYAL SOCIETY OF CHEMISTRY

www.rsc.org/advances

Graphical Abstract

A new cell permeable quinazoline based receptor (**1**) behaves as a highly selective and sensitive chemosensor for HSO_4^- ions of nanomolar region in aqueous medium by the formation of a survelion as $[LHSO_4]^-LH^+.3H_2O$ confirmed by single crystal X-ray crystallography.

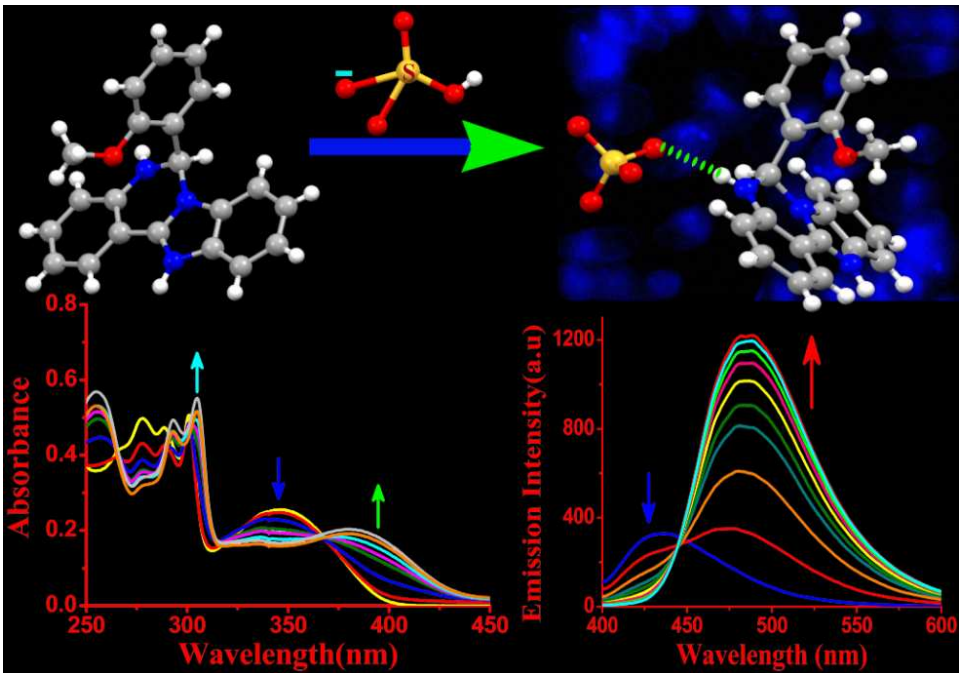

Cite this: DOI: 10.1039/c0xx00000x

www.rsc.org/xxxxxx

ARTICLE TYPE

A bio-attuned ratiometric hydrogen sulfate ion selective receptor in aqueous solvent: structural proof of the H-bonded adduct

Manjira Mukherjee,[a] Buddhadeb Sen,[a] Siddhartha Pal,[a] Samya Banerjee,[b] Somenath Lohar,[a] Ennio Zangrando,[c] and Pabitra Chattopadhyay*[,a]

Received (in XXX, XXX) Xth XXXXXXXXX 20XX, Accepted Xth XXXXXXXXX 20XX
DOI: 10.1039/b000000x

A new cell permeable quinazoline based receptor (**1**) selectively senses HSO_4^- ions of nanomolar region in 0.1 M HEPES buffer (ethanol/water:1/5, v/v) at biological pH over other competitive ions through the proton transfer followed by hydrogen bond formation and subsequent anion coordination to yield the $[LHSO_4]^-LH^+.3H_2O$ (**2**) ensemble, which has been crystallographically characterised to ensure the structure property relationship. This non-cytotoxic HSO_4^- ion selective biomarker is highly potential to recognize the intercellular distribution of HSO_4^- ions in HeLa cells under fluorescence microscope.

Introduction

In recent years development of selective and sensitive anionic receptors have gained significant attention because of the biological significance of the field, potential applications in sensors and the development of phase transfer reagents.[1,2] Critical physiological processes are being functioned through negative ion gradients across lipid bilayer membranes originated by anion channels.[3] The breakdown of this process leads to severe diseases such as cystic fibrosis, nephrolithiasis, osteopetrosis, Angelman's syndrome and Bartter's syndrome type III.[4] Among the various anions, hydrogen sulfate (HSO_4^-) ions dissociate at high pH to generate toxic sulfate (SO_4^{2-}), causing irritation of skin and eyes and even respiratory paralysis.[5] Despite its crucial roles in biological processes, only few examples of cell permeable HSO_4^- ions sensors have been reported.[6] Sensors based on anion-induced changes in fluorescence are particularly striking due to the simplicity, high degree of specificity and low detection limits.[7] Again, from the experimental point of view, it is also well known that the ratiometric fluorescence signalling, which involves measurement of the changes in the ratio of the optical response at two different wavelengths, is more attractive because the ratio between the two emission intensities can provide a built-in correction for environmental effects and stability under illumination.[8] However, the literature survey[6] revealed that the structure property relationship is still unexplored in all reports of HSO_4^- ion selective ratiometric/single point receptors.

Herein, a newly designed efficient receptor, *6-(2-methoxy-phenyl)-5,6-dihydro-benzo[4,5]imidazo [1,2c]quin-azoline,* L (**1**) which behaves as a ratiometric chemosensor selective for HSO_4^- ions at biological pH in ethanol-water HEPES buffer (1/5) (v/v) medium. The formation of an ensemble formulated as $[LHSO_4]^-LH^+.3H_2O$ (**2**) was confirmed by single crystal X-ray crystallography. Interestingly, other competitive anions such as F^-, Cl^-, Br^-, I^-, AcO^-, $H_2PO_4^-$, N_3^- and ClO_4^- etc. do not affect the selectivity of **1**. The probe **1** was also employed to detect the presence of intracellular bisulfate ion by acquiring the images of HeLa cells under a fluorescence microscope.

Experimental

Materials and physical measurements

All of the solvents were of analytical grade. The elemental analyses (C, H and N) were carried out on a Perkin Elmer 2400 CHN elemental analyzer. For recording electronic spectra, a Shimadzu (model UV-1800) spectrophotometer was used. IR spectra were recorded using Prestige-21 SHIMADZU FTIR spectrometer preparing KBr disk. ^{1}HNMR spectrum of organic moiety was obtained on a JEOL 400 spectrometer using DMSO-d_6 solution. Electrospray ionization (ESI) mass spectra were recorded on a Qtof Micro YA263 mass spectrometer. A Systronics digital pH meter (model 335) was used to measure the pH of the solution and the adjustment of pH was done using either 50 mM HCl or NaOH solution. Steady-state fluorescence emission and excitation spectra were recorded with a Hitachi-4500 spectrofluorimeter. Time-resolved fluorescence lifetime measurements were performed using a HORIBA JOBIN Yvon picosecond pulsed diode laser-based time-correlated single-photon counting (TCSPC) spectrometer from IBH (UK) at λ_{ex}= 370 nm and MCP-PMT as a detector. Emission from the sample was collected at a right angle to the direction of the excitation beam maintaining magic angle polarization (54.71).

The full width at half-maximum (FWHM) of the instrument response function was 250 ps, and the resolution was 28.6 ps per channel. Data were fitted to multi exponential functions after de convolution of the instrument response function by an iterative reconvolution technique using IBH DAS 6.2 data analysis software in which reduced w2 and weighted residuals serve as parameters for goodness of fit.

The fluorescence property of the sensor was investigated in water : ethanol (5:1, v/v) solvent. The pH study was done in 100 mM HEPES buffer solution by adjusting pH with HCl or NaOH. The stock solutions (~ 10^{-2} M) for the selectivity study of the receptor **1** towards different anions were prepared taking sodium perchlorate and azide, disodium hydrogen arsenate, tetra butyl ammonium salt of chloride, bromide, iodide, acetate, fluoride, dihydrogen phosphate and hydrogen sulfate ion; in water : ethanol (5:1, v/v) solvent. In this selectivity study the amount of these anions was a hundred times greater than that of the receptor used. Fluorescence titration was performed with hydrogen sulfate ions in water : ethanol (5 : 1, v/v) solvent varying the anion concentration from 0 to 100 μM with a receptor concentration of 25 μM.

Synthesis of 6-(2-methoxy-phenyl)-5,6-dihydro-benzo [4,5]imidazo[1,2c]quinazoline (1)

Preparation of the receptor **1** was carried out following a common procedure. *2-(2-aminophenyl)-benzimidazole* (2.09 g, 10.0 mmol) and *2-methoxy benzaldehyde* (1.36 g, 10.0 mmol) were mixed in dry ethanol (25.0 mL) at room temperature. Then the reaction mixture was continued to reflux for 6 h. The brown precipitate of the compound was obtained from the solution through slow evaporation of the solvent. The pure recrystallized compound was isolated from methanol.

$C_{21}H_{17}N_3O$ (1): Anal. Found: C, 76.81; H, 5.15; N, 13.07; Calc.: C, 77.03; H, 5.24; N, 12.84. ESI-MS: $[M + H]^+$, m/z, 328.1246 (100 %) (calcd.: m/z, 328.14; where M = molecular weight of **1**]; IR(cm^{-1}) : ν_{NH} = 3194.12, $\nu_{C=N}$ = 1616.35; ^{1}H NMR (δ, ppm in dmso-d_6): 7.98 (d, 1H, J = 7.6); 7.67 (d, 1H, J = 7.6); 7.29-7.15 (m, 5H); 7.10-7.05 (m, 3H); 6.87(d, 1H, J= 7.6); 6.80 (t, 1H, J= 7.6); 6.73 (t, 1H, J= 7.6); 6.60 (d, 1H, J= 7.6); 3.89(s, 1H). Yield: 90%.

Preparation of compound $[LHSO_4]^-LH^+.3H_2O$ (2)

The preparation of the complex adduct was carried out following a common procedure. To an ethanolic solution of **1** (327 mg, 1.0 mmol), the aqueous ethanolic solution of hydrogen sulfate ions was added and then the mixture was stirred at room temperature for 6 h. Then the solution obtained was kept aside for slow evaporation at room temperature. After a few days, deep yellow colored crystals of **2** were collected by washing with water and methanol, and then dried in vacuo. This crystalline compound was used for all the experimental works.

$[LHSO_4]^-LH^+.3H_2O$: $C_{42}H_{42}N_6O_9S$ (2): Anal. Found: C, 62.35; H, 5.94; N, 10.31; Calc.: C, 62.52; H, 5.25; N, 10.42. ESI-MS in methanol: $[M + Na + H]^+$, m/z, 448.2056 (obsd. with 6.89 % abundance) (calcd.: m/z, 448.089); where M = $[LHSO_4]^-$; IR(cm^{-1}) : $\nu_{S=O}$ = 1118.71, ^{1}H NMR (δ, ppm in dmso-d_6): 7.98 (d, 1H, J = 7.6); 7.86 (s,1H); 7.76 (d, 1H, J = 7.6); 7.52 (s,1H); 7.42-7.20 (m, 5H); 7.15-7.07(m, 2H); 6.90-6.86 (m, 3H); 3.70 (s, 1H). Yield: 75 %.

X-ray data collection and structural determination

Single crystals of **2** suitable for X-ray crystallographic analysis were obtained from a methanolic solution of **1** and hydrogen sulfate ions on slow evaporation at room temperature. Intensity data were collected using Mo-K_α (λ = 0.71073 Å) radiation on a SMART APEX II diffractometer equipped with CCD area detector. Cell refinement, indexing and scaling of the data set were carried out using the software package of SMART APEX II. A total of 21422 reflections were measured out of which 2290 were independent and 1674 were observed [$I > 2\sigma(I)$]. The structure was solved by direct methods using SHELXS-97[9] and refined by full-matrix least squares refinement methods based on F^2, using SHELXL-97.[9] All non-hydrogen atoms were refined anisotropically. The H atoms were fixed at calculated positions, those at N1 and N3 were located in the difference Fourier map and refined with thermal factor = 1.2 times of Ueq(N). Two residuals in the electron density map were interpreted as water oxygen atoms (one at half occupancy for which no H atoms were located). All calculations were performed using Wingx package.[10] Crystal data and details of refinement are given in **Table 1S** and a selection of bond lengths and angles is tabulated in **Table 2S**.

Preparation of cell and *in vitro* cellular imaging

Human cervical cancer cells HeLa were used for the cytotoxicity study. Cell were cultured in Dulbecco's modified Eagle's medium (DMEM, Gibco BRL) supplemented with 10% FBS (Gibco BRL), and 1% antibiotic mixture containing penicillin, streptomycin and neomycin (PSN, Gibco BRL), at 37 °C in a humidified incubator with 5% CO_2. The cells were grown to 80-90 % confluence, harvested with 0.025 % trypsin (Gibco BRL) and 0.52 mM EDTA (Gibco BRL) in PBS (phosphate-buffered saline, Sigma Diagnostics) and plated at desired cell concentration and allowed to re-equilibrate for 24 h before any treatment. Cells were rinsed with PBS and incubated with DMEM-containing **1** (10 μM, 1% DMSO) for 15 min at 37 °C. All experiments were conducted in DMEM containing 10% FBS and 1% PSN antibiotic. The imaging system was composed of a fluorescence microscope (ZEISS Axioskop 2 plus) with an objective lens [10X].[11]

Cell Cytotoxicity Assay

To test the cytotoxicity of **1**, MTT [*3-(4,5-dimethyl-thiazol-2-yl)-2,S-diphenyl tetrazolium bromide*] assay was performed following the reported procedure.[12] After treatments of the probe (5, 10, 25, 50, and 100 μM), 10 μl of MTT solution (10 mg/ml PBS) were added in each well of a 96-well culture plate and incubated at 37 °C for 8 h. All mediums were removed from wells and replaced with 100 μl of acidic isopropanol. The formed intracellular formazan crystals (blue-violet) were solubilized with 0.04 N acidic isopropanol and the absorbance of the solution was measured at 595 nm wavelength with a microplate reader. Values are means ± S.D. of three independent experiments. The cytotoxicity of **1** was calculated as percentage of cell viability.

Theoretical Calculation

To clarify the configurations and H-bonding feature of the host (**1**) and guest-host species (**[$LHSO_4$]$^-$**), DFT calculations were performed using **Gaussian-09** software over a Red Hat Linux IBM cluster. Molecular level interactions between **1** and **2** have been studied using density functional theory (DFT) with the **B3LYP/6-31G(d,p)** functional model and basis set.

Results and discussion

Synthesis and characterization

The organic moiety (**1**) was synthesized by condensing an ethanolic solution of *2-(2-aminophenyl)-benzimidazole* with *2-methoxybenzaldehyde* in 1:1 mole ratio (Scheme 1, Supporting Information). It was characterized by physico-chemico and spectroscopic tools. The peaks obtained in the ^{1}H NMR spectrum of **1** in solution have been assigned and these are in accordance with the proposed structural formula (Fig. S1, Supporting Information). The ESI mass spectrum of **1** in methanol showed a peak at m/z 328.1246 with 100 % abundance assignable to $[M + H]^+$ (calculated value at m/z, 328.14) where M = molecular weight of **1** (Fig. S2, Supporting Information). IR spectra of **1** showed the characteristic stretchings assignable to ν_{N-H} and $\nu_{C=N}$ (Fig. S3, Supporting Information).

The formation of adduct between the organic species and HSO_4^- ion was established by single crystal X-ray structural analysis. The reaction of one mole hydrogen sulfate ions with one mole of the organic moiety in methanol at stirring condition led to a compound formulated in solid state as $[LHSO_4]^-.LH^+.3H_2O$ (**2**). This ensemble **2** is soluble in methanol, DMSO, acetonitrile. The ^{1}H NMR peaks of **2** dissolved in DMSO-d_6 are consistent with the structural formula obtained in solid state Fig. S4, Supporting Information. A peak at m/z, 448.2056 in the ESI mass spectrum in methanol (Fig. S5, Supporting Information) and the characteristic stretching at 1119 cm^{-1} observed in the IR spectra attributable to $\nu_{S=O}$ (Fig. S6, Supporting Information) confirm the presence of hydrogen sulfate ions attached to **1** to form the compound formulated in solid state as $[LHSO_4]^-LH^+.3H_2O$ (**2**). In fact, the solid state structure of **2** was established by single crystal X-ray crystallography. A molecular view of the $[(LH)SO_4]^-$ moiety of **2** with atom labelling scheme is shown in Fig. 1.The crystallographic data and bond parametersof **2**, which crystallizesin the monoclinic space group *C*2/c, are tabulated in Tables S1 and S2. In the five-membered ring the N1-C16 bond distance(1.397(5) Å) is slightly longer than those of N1-C15 (1.335(5) Å) and N2-C15 (1.347(5) Å), thus indicating a considerable double bond character in these. Moreover it is of interest the difference observed between the N3-C9 and N3-C8 bond lengths of 1.363(5) and 1.465(5)Å, respectively. The RX structural determination clearly evidences the position of the hydrogens at N1 and N3 in the heterocycle rings. Crystal packing of **2** shows each sulfateoxygen atom involved in H-bond with a NH group of four symmetry related organic molecules (Fig. 2a), being the sulfur located on a crystallographic two fold axis running from top to down in the picture. These interactions give rise to a polymeric chain (Fig. S7). Moreover the molecules are paired in the cell about a center of symmetry through π-π interactions occurring between rings N1/C15/N2/C21/C16 and C9/C10/C11/C12/C13/C14 (Fig. 2b, centroid-to centroid distance of 3.70 Å).

^{1}HNMR titration in DMSO-d_6 ensured the formation of the species **2** in solution state (Fig. S8, Supporting Information). The peak appeared at δ 7.86 in the spectrum of $[LHSO_4]^-LH^+$ complex in DMSO-d_6 corresponds to imidazolic N-H proton. The signals at 6.6, 6.73 [H_h and H_g protons] of **1** shifted towards downfield and merge with $H_{g'}$ and appeared as 3H equivalent multiplate at around δ 6.89. The other signals for corresponding protons assure the presence of the probe in **2**. To confirm the peak for the NH proton, ^{1}HNMR spectra of both **1** and **2** were also obtained using D_2O solvent (Figs. S9 and S10, Supporting Information). Due to the addition of D_2O into DMSO-d_6 solution of **1**, the peaks of H_g and H_h broadens and NH peak disappeared; in the similar type of experiment in case of **2**, disappearance of the peaks for both NH protons of 5 and 6 membered rings was observed .

Spectral characteristics

Absorption study

The UV-vis spectrum of **1** showed the characteristic absorption bands at 277, 290 and 348 nm. In similar experiment, addition of HSO_4^- ions to the colourless solution of **1** in ethanol-water (1 : 5, v/v) HEPES buffer (0.1 M, pH 7.4) at 25 °C, the peak at 348 nm was red shifted to a new peak at 385 nm (Fig. 3) through an isosbestic point at 367 nm due to the formation of the adduct (**2**) in solution.

Emission study

On excitation at 390 nm, the probe **1** showed fluorescence at 430 nm (Figs. S11 and S12, Supporting Information). Gradual addition of HSO_4^- ions (0-30 μM) to **L** (25 μM) causes gradual decrease of the fluorescence intensity at 430 nm with concomitant increase of a new band at ca. 485 nm through an isoemissive point at 445 nm (Fig. 4). The ratiometric enhancement at 485 nm (*ca.* 8.34 times) is in agreement of seven times increase in quantum yield estimated by integrating the area under the fluorescence curves with the equation:

$$\phi_{sample} = \frac{OD_{standard} \times A_{sample}}{OD_{sample} \times A_{standard}} \times \phi_{standard}$$

where A is the area under the fluorescence spectral curve and OD is the optical density of the compound at the excitation wavelength. The standard used for the measurement of fluorescence quantum yield was anthracene (Φ = 0.29 in ethanol).

The ratiometric signalling of fluorescence output at two different wavelengths plotted as a function of concentration of HSO_4^- ions shows that the fluorescence intensity ratio at wave length 485 and 430 nm (I_{485}/I_{430}) gradually increases following with augment of the concentration of HSO_4^- ions (Fig. S13, Supporting Information) and after a certain time it levels up to produce a sigmoid curve.

Here, a slight blue fluorescence in **1** was observed due to the PET process occurring from *benzimidazole* to *o-anisyl* unit with a low probability due to the presence of the *methoxy* group (+R effect).[6d] On gradual addition of HSO_4^- ions to **1**, the protonation has been occurred at the donor imidazolic-N end, which helped to block the PET process by reducing the electron availability in the donor end (imidazolic-N atom) (Scheme 2). As a result, a significant enhancement of fluorescence intensity was observed due to the interaction of **1** with HSO_4^- ion at the quinazoline-N end through intermolecular hydrogen bonding assisted CHEF process. As this type of enhancement was not observed by adding sulfate anion in experiment at same condition, it may be concluded that HSO_4^- ions help the imidazole-N to be protonated and in turn deprotonation of HSO_4^- ions favours the interaction with quinazoline-H, similarly to the earlier report.[6a]

The fluorescence response of the organic moiety towards different anions, namely Cl^-, Br^-, I^-, F^-, CN^-, OAc^-, NO_3^-, S^{2-}, SO_4^{2-}, $H_2PO_4^-$, $H_2AsO_4^-$ and HSO_4^-, was also investigated. In this study the concentration of the anions was 100 times greater than **1** and the results, reported in Figs. S14 and S15 (Supporting Information), indicate that **1** has tremendous selectivity towards HSO_4^- over other anions. The fluorescence intensity of the organic compound remained unchanged over the range of pH 5.0-12.0 in absence of HSO_4^- ions. The fluorescence intensity of the organic moiety in presence of HSO_4^- ions was considerably higher with respect to that observed for the HSO_4^- ion free receptor **1** (Fig. S16, Supporting Information) due to the formation of the H-bonded adduct described above. At higher pH values (8.0-12.0), the gradual decrease of the fluorescence intensity is due to a reduced formation probability of the adduct between HSO_4^- ions with the receptor since there is a tendency of HSO_4^- to be deprotonated. There was almost no interference for the detection of HSO_4^- ions in presence of 100 equivalent concentrations of tetrabutylammonium salt of chloride, bromide, iodide and acetate; sodium salt of azide, sulphide, cyanide, dihydrogen phosphate and dihydrogen arsenate; and potassium salt of nitrate and sulfate. Job's plot analysis reveals that the receptor **1** binds with HSO_4^- ions to form a 1:1 adduct (Fig. S17, Supporting Information). The binding constant value K, calculated from the emission intensity data, was found to be 1.648×10^5 M^{-1} (Fig. S18, Supporting Information) using the modified Benesi-Hildebrand equation corresponding to a 1:1 stoichiometry.[13]

$$1/(F_x-F_0)=1/(F_{max}-F_0)+(1/K[C])(1/(F_{max}-F_0)$$

where F_0, F_x, and F_{max} correspond to the emission intensities of the organic moiety in the absence of HSO_4^- ions, at an intermediate HSO_4^- concentration, and at a concentration of complete interaction, respectively, and [C] represents the HSO_4^- concentration. This study indicates the strong binding affinity and high selectivity of **1** towards HSO_4^- ions.

As a result of this observation, the probe is very effective to be used as sensors in analytical and bioanalytical studies, which were carried out at biological pH in ethanol-water (1 : 5, v/v) HEPES buffer (0.1 M) at 25 °C. The detection limit was also estimated to be 28.72 nM (Fig. S19, Supporting Information) calculated using the equation $3\sigma/S$.[14]

The fluorescence average lifetime measurement of **1** in presence and absence of HSO_4^- ion in the water-ethanol (5 : 1) medium indicates a gradual increase by increasing the $[HSO_4^-]$ (Fig. S20, Supporting Information). The average lifetime for **1** is 9.038 ns and in case of **1** : HSO_4^- ratio of 1:1, the lifetime is 12.76 ns. According to the equations: $\tau^{-1} = k_r + k_{nr}$ and $k_r = \Phi_f/\tau$,[15] the radiative rate constant k_r and total non-radiative rate constant k_{nr} of the organic moieties were tabulated in Tables S3. The data suggest that the fluorescent enhancement is ascribed to the decrease of the k_{nr}/k_r ratio from 13.35 for **1** to1.001 for $[LHSO_4]^-$. The stability of complex can also be supported by the computational study of **1** and its corresponding HSO_4^- adduct (**Fig. S21**). The narrowing of the energy gap between the HOMO and LUMO of $[LHSO_4]^-$ compared to L demonstrated the facile conversion as well as the extra stability of the $[LHSO_4]^-$.

Analytical figure of merit

The detection limit was calculated from the calibration curve based on the fluorescence enhancement at 485 nm **(**Fig. S19, Supporting Information) focusing on the lower concentration region of HSO_4^- ion. From the slope of the curve (S) and the standard deviation of seven replicate measurements of the zero level (σ_{zero}), the detection limit was estimated using the equation $3\sigma/S$. The data from this graph indicate that this probe effectively detects HSO_4^- ions at very low level concentration (LOD = 28.72 nM).

Cell Imaging

To examine the utility of the probe in biological systems, it was tested towards human cervical cancer HeLa cell. Here, HSO_4^- and **1** were allowed to be uptaken by the cells of interest and the images of the cells were recorded by fluorescence microscopy following excitation at ~390 nm (Fig. 5). In addition, the *in vitro* study showed that 50 μM of **1** was not cytotoxic to cell up to 18.0 h (Fig. S22, Supporting Information).This results indicate that the probe has a potentiality as HSO_4^- sensor for both *in vitro* and *in vivo* application as well as imaging in different ways as same manner for live cell imaging can be followed instead of fixed cells.

Conclusion

In conclusion, a new quinazoline based HSO_4^- ion selective receptor has been developed with the help of detailed experimental studies that show the enhancement of fluorescence after addition of HSO_4^- ions. Single crystal X-ray crystallography allowed to ascertain the detailed structure of the produced ensemble of the receptor with HSO_4^- ion formulated as $\mathbf{[LHSO_4]^-LH^+.3H_2O}$. This non-cytotoxic probe is useful for the detection of intracellular HSO_4^- ions in HeLa cells.

Acknowledgements

Financial assistance from CSIR, New Delhi, India is gratefully acknowledged. M. Mukherjee wishes to thank to UGC, New Delhi, India for offering the fellowship. We sincerely acknowledge Prof. B. Mukhopadhyay, IISER, Kolkata for providing the facility to record NMR spectra; Prof. Samita Basu and Mr. Ajay Das, Chemical Science Division, SINP, Kolkata for enabling TCSPC facility. The authors sincerely thank to USIC, B.U. for the single crystal X-ray diffractometer facility under PURSE program. The authors are grateful to the honorable reviewers for their valuable comments.

Notes and references

[a]*Department of Chemistry, Burdwan University, Golapbag, Burdwan-713104, West Bengal, India, E-mail: pabitracc@yahoo.com*
[b]*Department of Inorganic and Physical Chemistry, Indian Institute of Science, Bangalore, 560012, India*
[c] *Dipartimento di Scienze Chimiche e Farmaceutiche, Via Licio Giorgieri 1, 34127 Trieste, Italy*

†Electronic Supplementary Information (ESI) available: See DOI: 10.1039/b000000x/

‡CCDC 1007155 contains the supplementary crystallographic data for this paper. These data can be obtained free of charge from The Cambridge Crystallographic Data Centre *via* http://www.ccdc.cam.ac.uk/data_request/cif.

(1) (a) L. E. Santos-Figueroa, M. E. Moragues, E. Climent, A. Agostini, R. Martınez-Manez and F. Sancenon, *Chem. Soc. Rev.,* 2013, **42**, 3489; (b) M. Wenzel, J. R. Hiscock and P. A. Gale, *Chem. Soc. Rev*., 2012, **41**, 480; (c) R. M. Duke, E. B. Veale, F. M. Pfeffer, P. E. Kruger and T. Gunnlaugsson, *Chem. Soc. Rev.*, 2010, **39**, 3936; (d) E. J. O'Neil and B. D. Smith, *Coord. Chem. Rev.*, 2006, **250**, 3068.

(2) (a) R. A. Potyrailo, V. M. Mirsky, *Combinatorial Methods for Chemical and Biological Sensors*, Springer, 2009; (b) C. Tan, Q. Wang and L. Ma, *Photochemistry and Photobiology,* 2010, **86**, 1191; (c) T. Y. Joo, N. Singh, G. W. Lee and D. O. Jiang, *Tetrahedron Lett.*, 2007, **48**, 8846; (d) S. E. Matthews and P. D. Beer, *Supramol. Chem.*, 2005, **27917**, 411.

(3) (a) F. M. Ashcroft, Ion Channels and Disease Channelopathies, Academic Press, San Diego, 2000; (b) V. Gorteau, G. Bollot, J. Mareda, A. Perez-Velasco and S. Matile, *J. Am. Chem. Soc*., 2006, **128**, 14788; (c) A. P. Davis, D. N. Sheppard and B. D. Smith, *Chem. Soc. Rev.*, 2007, **36**, 348.

(4) (a) T. J. Jentsch, C. A. Hubner and J. C. Fuhrmann, *Nat. Cell Biol*., 2004, **6**, 1039; (b) T. J. Jentsch, T. Maritzen, A. Zdebik, A.*, J. Clin. Invest*., 2005, **115**, 2039.

(5) P. I. Jalava, R. O. Salonen, A. S. Pennanen, M. S. Happo, P. Penttinen, A. I. Halinen, M. Sillanpaa, R. Hillamo and M. R. Hirvonen, *Toxicol. Appl. Pharmacol.*, 2008, **229,** 146.

(6) (a) M. Alfonso, A. Tarraga, and P. Molina , *Org. Let.,* 2011, **13**, 6432; (b) V. Kumar, A. Kumar, U. Diwan and K. K. Upadhyay, *Chem. Commun.,* 2012, **48**, 9540; (c) W. Lu, J. Zhou, K. Liu, D. Chen, L. Jiang and Z. Shen , *J. Mater. Chem. B.,* 2013, **1**, 5014; (d) M. Mukherjee, S. Pal, B. Sen, S. Lohar, S. Banerjee, S. Banerjee and P. Chattopadhyay, *RSC Adv.,* 2014, **4**, 27665; (e) L. Wang, L. Yang and D. Cao, *J. Fluoresc*., 2014, **24**, 1347; (f) D. Sarkar, A. K. Pramanik and T. K. Mondal, *RSC Adv.,* 2014, **4**, 25341; (g) B. Sen, M. Mukherjee, S. Pal, S. K. Mandal, M. S. Hundal, A. R. Khuda-Bukhsh and P. Chattopadhyay, *RSC Adv.,* 2014, **4**, 15356 and refs. therein.

(7) (a) S. Sen, M. Mukherjee, K. Chakrabarty, I. Hauli, S. K. Mukhopadhyay and P. Chattopadhyay, *Org. Biomol. Chem.*, 2013, **11**, 1537; (b) Z. Yang, K. Zhang, F. Gong, S. Li, J. Chen, J. S. Ma, L. N. Sobenina, A. I. Mikhaleva, G. Yang and B. A.Trofimov, *Beilstein J. Org. Chem.,* 2011, **7**, 46; (c) S. K. Kim, D. H. Lee, J. I. Hong and J. Yoon, *Acc. Chem. Res*., 2009, **42**, 23; (c) C. H. Lee, H. Miyaji, D. W. Yoon and J. L. Sessler, *Chem. Commun*., 2008, 24; (d) X. Huang, Z. Guo, W. Zhu, Y. Xie and H. Tian, *Chem. Commun*., 2008, 5143; (e) T. Gunnlaugsson, M. Glynn,. G. M. Tocci, P. E. Kruger and F. M. Pfeffer, *Coord. Chem. Rev*., 2006, **250**, 3094;

(8) (a) Z. Xu, Y. Xiao, X. Qian, J. Cui and D. Cui, *Org. Lett*., 2005, **7**, 889; (b) B. Valeur, and I. Leray, *Coord. Chem. Rev.*, 2000, **205**, 3; (c) S. Sen, S. Sarkar, B. Chattopadhyay, A. Moirangthem, A. Basu, K. Dhara and P. Chattopadhyay, *Analyst*, 2012, **137**, 3335.

(9) G. M. Sheldrick, *Acta Cryst A*, 2008, **A64**, 112-122

(10) L. J. Farrugia *J. Appl. Cryst,* 1999*,* **32**, 837.

(11) J. L. McClintock and B. P. Ceresa, 2010, **51,** 3455.

(12) (a) S. Banerjee, P. Prasad, A. Hussain, I. Khan, P. Kondaiah, A. R. Chakravarty, *Chem. Commun.*, 2012, ***48***, 7702. (b) T. Mosmann *J. Immunol. Methods*.,1983, **65**, 55.

(13) H. A. Benesi, J. H. Hildebrand, *J. Am. Chem. Soc.,* 1949, **71**, 2703.

(14) (a) A. Hakonen, *Anal. Chem*., 2009, **81,** 4555; (b) S. Pal, B. Sen, M. Mukherjee, K. Dhara, E. Zangrando, S. K. Mandal, A. R. Khuda-Bukhsh and P. Chattopadhyay, *Analyst*, 2014, **139**, 1628.

(15) N. J. Turro, *Modern Molecular Photochemistry*, Benjamin/ Cummings Publishing Co., Inc., Menlo Park, CA, 1978, p. 246.

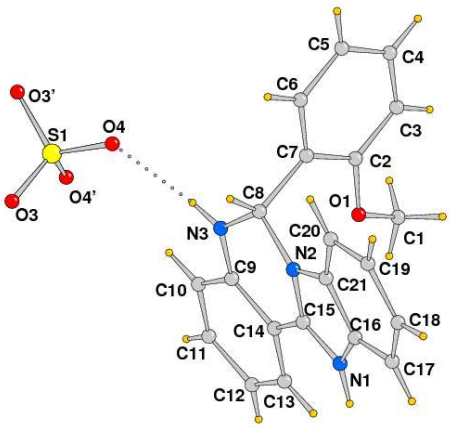

Fig. 1 Molecular structure of the $[LHSO_4]^-$ moiety with atom numbering scheme. The sulfur is located on a crystallographic two fold axis.

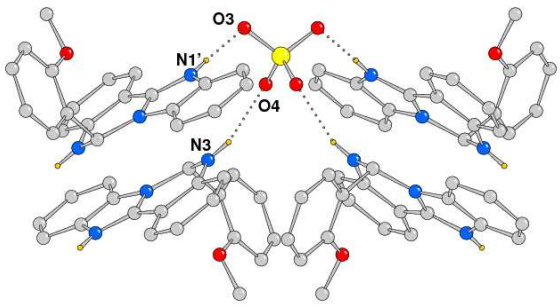

Fig. 2a Crystal packing of compound **2** (water molecules not displayed for clarity) showing H-bonds involving sulfate oxygen atoms with NH groups [N(1')...O(3) 2.699(2) Å, N(1')-H 0.91 Å, N(1)-H…O(3) 167°; N(3)...O(4) 2.866(2) Å, N(3)-H(3N) 0.98 Å, N(3)-H…O(4) 162°].

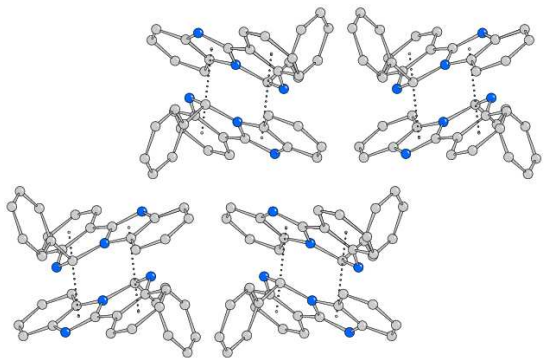

Fig. 2b Perspective view of the packing showing molecules paired about a center of symmetry through ππ interactions

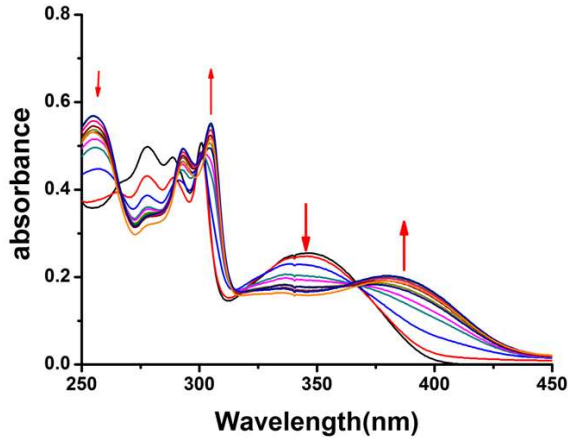

Fig. 3 Changes in the absorption spectra of **1** (25 μM) upon addition of 0-30 μM of HSO_4^- in ethanol-water (1 : 5, v/v) HEPES buffer (0.1 M, pH 7.4) at 25 °C.

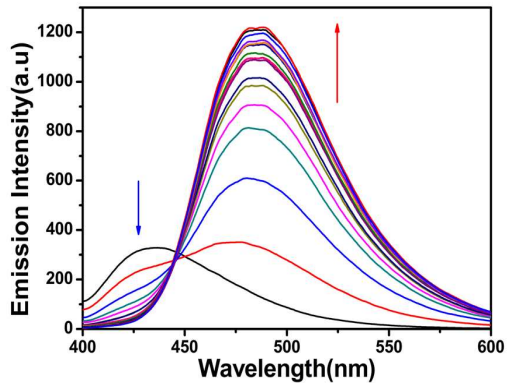

Fig. 4 Fluorescence spectra of **1** (25 μM) as a function of HSO_4^- ion concentration [0-30 μM] in ethanol-water (1 : 5, v/v) HEPES buffer (0.1 M, pH = 7.4) at 25 °C [λ_{em}: 485 nm, λ_{ex} = 390 nm].

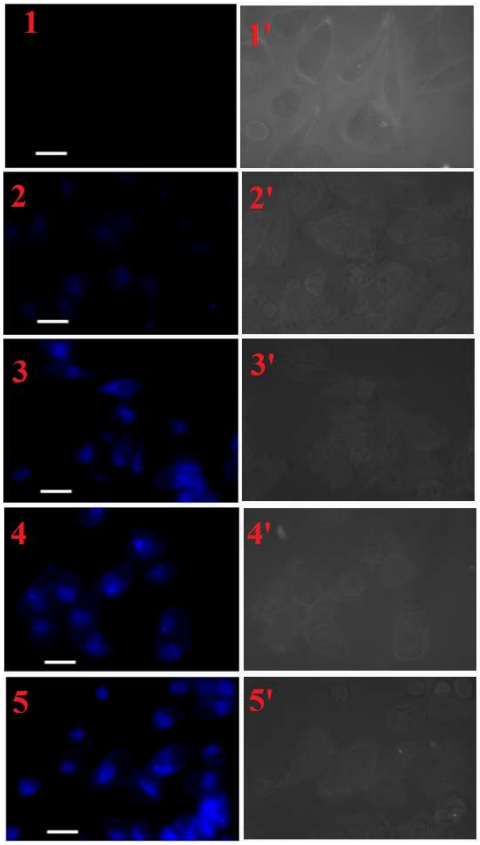

Fig. 5 Phase contrast (right) and fluorescence images (left) of HeLa cells after incubation with **1** in presence of hydrogen sulfate ions (1, 1′) 0 μM, (2, 2′) 3 μM, (3, 3′) 5 μM, (4, 4′) 7 μM, and (5, 5′) 10 μM, respectively for 30 min at 37 °C.

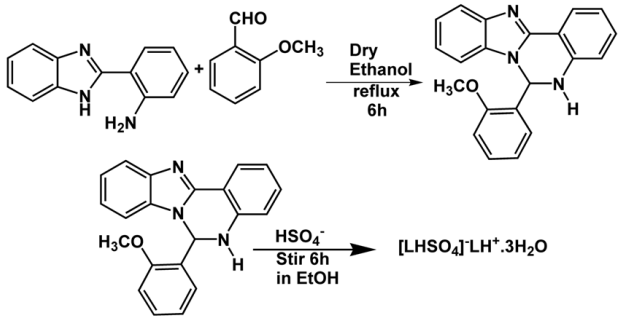

Scheme 1 Schematic representation of synthesis of the probe **L** (**1**) and **[LHSO$_4$]$^-$LH$^+$** (**2**)

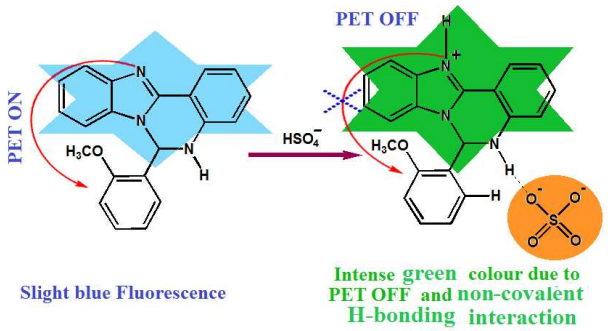

Scheme 2 Schematic representation of plausible mechanism of hydrogen sulfate sensing